Optical Fiber Systems Are Convectively Unstable

A. Mussot,[1,*] E. Louvergneaux,[1] N. Akhmediev,[2] F. Reynaud,[3] L. Delage,[3] and M. Taki[1]

[1]*Laboratoire de Physique des Lasers, Atomes et Molécules, UMR-CNRS 8523 IRCICA, Université des Sciences et Technologies de Lille, 59655 Villeneuve d'Ascq Cedex, France*

[2]*Optical Sciences Group, Research School of Physical Sciences and Engineering, The Australian National University, Canberra, ACT 0200, Australia*

[3]*Département photonique/IRO Xlim UMR6172, 123 rue A. Thomas, 87060 Limoges Cedex, France*

(Received 1 April 2008; published 11 September 2008)

We theoretically and experimentally evidence that fiber systems are convective systems since their nonlocal inherent properties, such as the dispersion and Raman effects, break the reflection symmetry. Theoretical analysis and numerical simulations carried out for a fiber ring cavity demonstrate that the *third-order dispersion* term leads to the appearance of convective and absolute instabilities. Their signature is an asymmetry in the output power spectrum. Using this criterion, experimental evidence of convective instabilities is given in a fiber cavity pumped by a pulsed laser.

DOI: 10.1103/PhysRevLett.101.113904 PACS numbers: 42.65.Sf, 05.45.−a, 42.55.Wd, 47.54.−r

Convective and absolute instabilities arising in temporal systems as well as in spatially extended systems are common to a class of nonlinear dynamical systems, namely, the convective ones. They form a platform of multidisciplinary research activities including, e.g., hydrodynamics [1], plasma physics [2], traffic flow [3], surface science [4], chemical reactions [5], and nonlinear optics [6–8]. It has been shown that the existence of convective instabilities in such systems gives rise to new and unexpected behaviors such as self-pulsing instabilities [8], pattern selection [9], and noise-sustained structures [1,9]. The key feature for the occurrence of such convective regimes in a system is the presence of *nonlocal* terms that break the reflection symmetry in the governing equations. In most nonlinear science modeling, these terms appear in the form of either *first-order* spatial or temporal derivative accounting for local couplings, or *distributed integrals* accounting for global couplings. The reflection symmetry breaking induced by these terms leads to convective and absolute instabilities, giving rise to asymmetric solutions. For instance, in spatially extended systems, convective regimes have been recently observed by tilting the feedback mirror in experiments on a liquid crystal with optical feedback [7], or, in temporal systems, by mismatching the synchronization of the pump pulses in fiber ring cavity experiments [8]. Thus, all systems whose models possess nonlocal terms that break the reflection symmetry are convective. Notice that this includes the huge number of amplitude equations as nonlinear Schrödinger, Ginzburg-Landau, and Swift-Hohenberg equations.

In this Letter, we show that fiber systems belong to the class of convective systems (see [10] for this classification) because they are mainly modeled by different forms of the extended nonlinear Schrödinger equation. The nonlocal terms stem from either higher order temporal derivatives (nonlocal coupling) or the Raman effect (global coupling). These terms provide both the reflection symmetry breaking and the traveling character for the spontaneous generation of convective instabilities. It turns out that optical fiber systems systematically exhibit convective and/or absolute regimes. We demonstrate here, by considering a fiber ring resonator, the generation of convective regimes for both cw and pulsed injected fields. More precisely, our analytical study predicts that the third-order dispersion term leads to the existence of two distinct instability thresholds, namely, the convective and absolute ones. Numerical simulations obtained by integrating the governing equations of the fiber cavity including boundary conditions confirm these predictions and show that the signature of convective regimes can be characterized by an asymmetry in the power spectrum of the output field [11]. Using this asymmetry as a criterion we have evidenced the experimental occurrence of convective instabilities in a fiber cavity pumped by a pulsed laser in complete agreement with the theory.

The system under investigation is a ring cavity whose nonlinear element is a fiber. Figure 1 depicts a simplified scheme of the experimental setup. A laser field with power $\|E_i\|^2$ is launched into the cavity through a beam splitter. At each round-trip the light inside the fiber is coherently superimposed with the input beam. The experimental device dynamics can be described by the extended nonlinear Schrödinger equation with boundary conditions as [12]

$$\partial_z E(z,\tau) = \left(-i\frac{\beta_2}{2}\partial_{\tau^2} + \frac{\beta_3}{6}\partial_{\tau^3} + i\gamma\int_{-\infty}^{+\infty} R(\tau')|E(z,\tau-\tau')|^2 d\tau'\right)E(z,\tau), \quad (1)$$

$$E(0,\tau + t_R) = TE_i(\tau) + \rho E(L,\tau)\exp(-i\Phi_0), \quad (2)$$

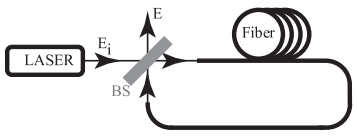

FIG. 1. Experimental setup. BS, beam splitter.

with t_R being the round-trip time which is the time it takes for a pulse to travel the cavity length L with the group velocity, Φ_0 the linear phase shift, T^2 (ρ^2) the mirror intensity transmissivity (reflectivity), and L the cavity length. The electric field inside the cavity is denoted E. $\beta_{2,3}$ are the second- and third-order dispersion terms, respectively. γ is the nonlinear coefficient, z the longitudinal coordinate, τ the time in a reference frame moving at the group velocity of the light, and $R(\tau')$ the nonlinear response including both instantaneous (Kerr effect) and delayed contributions (Raman effect). To study the role of the nonlocal terms (odd-order dispersion and Raman effect) in the generation of convective regimes, and to keep mathematics as simple as possible, we perform the reduction of the above infinite-dimensional map [Eqs. (1) and (2)] into the following modified Lugiato-Lefever equation that has been proven to be relevant for describing weakly nonlinear dynamics in the fiber cavity [12]. It reads

$$\frac{\partial\psi}{\partial t'} = S - (1 + i\Delta)\psi - i\beta_2\frac{\partial^2\psi}{\partial\tau'^2} + B_3\frac{\partial^3\psi}{\partial\tau'^3} + i\psi\int_{-\infty}^{+\infty} R(\tau'')|\psi(\tau' - \tau'')|^2 d\tau'', \quad (3)$$

where $t' = t(T/2t_R)$ with t the real time, $\tau' = \tau(T^2/L)^{1/2}$, $\psi = E\sqrt{2\gamma L/T^2}$, $S = 2/T(2\gamma L/T^2)^{1/2}E_i$, $B_3 = \beta_3 T/\sqrt{9L}$, and $\Delta = 2\Phi_0/T^2$. Here we neglect the Raman contribution but keep the Kerr effect and carry out the analytical study for configurations where the dispersion slope (β_3) influence is significant as compared to the lower order dispersion term. This assumption corresponds to a configuration where the frequency of instability is close enough to the pump carrier frequency, so that the Raman gain or absorption value is negligible compared to the modulational instability (MI) one. The steady state response ψ_s of Eq. (3) satisfies $S_s = [1 + i(\Delta - I_s)]\psi_s$, where $I_s = |\psi_s|^2$. Starting from the above equation, we can perform a linear stability analysis that provides us with the convective and absolute thresholds peculiar to convective systems. Assuming perturbations of the stationary state in the form $\exp i(Q\tau' - \Omega t')$, the following dispersion relation is obtained:

$$\Omega = -B_3Q^3 + i\{-1 + \sqrt{I_s^2 - (\Delta - \beta_2Q^2 - 2I_s)^2}\}. \quad (4)$$

Note that the role of the third-order dispersion on soliton propagation and radiation emission has been studied previously in Refs. [13–16]. Our present work shows the appearance of convective instability as a result of reflection symmetry breaking caused by β_3. The convective threshold is obtained by canceling the growth rate $\mathrm{Im}(\Omega(Q_c))$ of the most unstable mode Q_c. The absolute threshold is determined following the method of steepest descend [17]. It is reached when $\mathrm{Im}(\Omega(Q_s)) = 0$, where Q_s is a saddle point satisfying $d\Omega/dQ = 0$. These thresholds are plotted in Fig. 2 versus the dispersion slope parameter β_3. As can be seen from this figure, there exists a convective regime as soon as $\beta_3 \neq 0$. It is located between the convective and the absolute thresholds and increases monotonically with β_3. Although the third-order dispersion does not impact the onset of MI, it leads to the appearance of convective and absolute instabilities as it introduces a group velocity through the dispersion relation [first right-hand term in Eq. (4)]. The fact that the threshold does not depend on β_3 is not surprising. The main feature of a convective instability is not to necessarily impact the instability threshold but to give rise to a nonvanishing "group velocity" of the wave packet generated by small localized perturbations.

To check the values of these thresholds, we have performed numerical integrations of the infinite-dimensional map with boundary conditions [Eqs. (1) and (2)] using the split-step Fourier method. The determination of the convective and absolute thresholds is carried out by using the following well-known classical test for identifying the nature of instability: we initialize the system with a localized perturbation at time $t = 0$ and observe its evolution. Two dynamical behaviors are then developed: (i) the advection is "faster" than the growth of the initial local disturbance so that the system returns locally to its initial homogeneous steady state; (ii) the growth dominates the drift upstream so that the system reaches a modulated state. The first regime reveals the occurrence of a *convective instability* (CI) and the second one characterizes an *absolute instability* (AI). Consequently, we superimpose, at the first round-trip of integration, a small localized perturbation on the continuous wave pump with a frequency in the band of MI. This disturbance corresponds to a sine oscillation with a Gaussian envelope of short duration time (2 ps) and small amplitude (a few percent of the pump power). In the subsequent round-trips, only the continuous wave is injected. Then, the temporal evolution of this perturbation provides us the convective and the absolute nature of the regime. Typical temporal evolutions of the

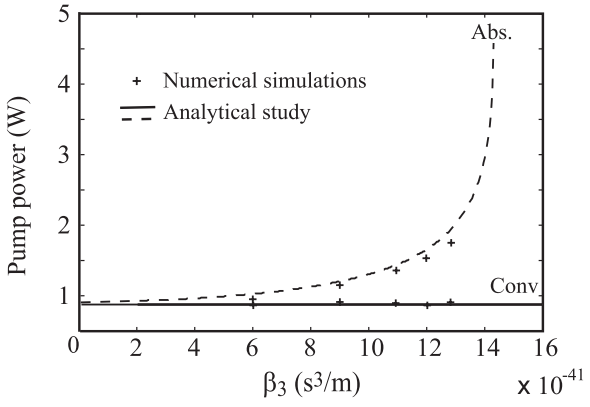

FIG. 2. Evolution of the convective and absolute thresholds versus the value of the dispersion slope. $\beta_2 = -5 \times 10^{-28}$ s^2/m, $\gamma = 2.5 \times 10^{-3}$ W^{-1} km^{-1}, $\Phi_0 = 0$, $L = 60$ m, $R = 0.8267$, and $T = 0.303$. These parameters correspond to a standard telecommunication fiber (with $\beta_3 = 1.2 \times 10^{-40}$ s^3/m).

perturbation are shown in Figs. 3(a) and 3(b) using a ''pseudospatiotemporal'' representation corresponding to the fast temporal evolution of the system in the comoving reference frame (horizontal axis) plotted at each round-trip (vertical axis). In other words, this is the slow time versus the fast time evolution. These diagrams clearly show the main characteristics of convective and absolute regimes (Figs. 3). For instance, the power evolution of the intracavity field at the fixed time value $\tau = 6.5$ ps demonstrates that for the convective regime the perturbation is amplified but the system locally returns back to the steady state value [Fig. 3(c)], whereas for the absolute regime the same perturbation leads to a stable modulated state [Figs. 3(b) and 3(d)]. In both cases a symmetry breaking in the temporal domain is observed during the evolution. From this analysis we got the numerical convective and absolute threshold values that fully confirm the analytical ones as can be seen in Fig. 2 (crosses). A striking feature appearing in Fig. 2 is the existence of a limit value $\beta_{3_{\mathrm{lim}}} \simeq 14.27 \times 10^{-41}$ s^2/m, over which the instabilities become purely convective. It means that under pulsed pumping, if no noise is present in the fiber system or on the input signal, no instability is able to develop in the system, even above the convective threshold. The initial input perturbations will first induce the rising up of MI and then disappear after some time due to the drift that will drive the oscillations below the CI threshold. On the contrary, in a noisy system, the instabilities will be sustained by noise and the two expected side bands will be observed in the output power spectrum. It is worth noting that with a cw pump the behavior is completely different and the observation of MI for $\beta_3 > \beta_{3_{\mathrm{lim}}}$ is possible whatever noise conditions are. Experimentally, the previous classical perturbation test is not accessible for two reasons. The most important reason is due to the presence of noise in the system, and the second one is due to the frequency band of the instability (few THz) that is well above the bandpass of photodetectors. The former one leads to noise-sustained oscillations in the regime of convective instability. As a result, propagating modulated states are observed in the pseudospatiotemporal mapping diagrams for both unstable regimes of CI and AI, but do not differ sufficiently to be distinguished without any ambiguity. Thus, in order to evidence the existence of CI and AI regimes, we look for a signature of these regimes based on the study of the output power spectrum features. We numerically found that in the convective regime an asymmetry is observed between the amplitudes of the two frequencies of instability [solid lines in Fig. 4(a)]. By increasing the pump power to reach the absolute regime we observed the same feature with an increase of the asymmetry [solid lines in Fig. 4(b)]. This asymmetry feature is a clear signature of the convective nature of the system since they disappear as soon as the slope of the dispersion vanishes ($\beta_3 = 0$) leading to a perfect symmetric spectrum [dotted lines in Figs. 4(a) and 4(b)]. Obviously, this is the case when the dispersion curve of the fiber is perfectly flat but also when the pump wavelength is very far from the zero dispersion wavelength of the fiber. In this latter case, the frequencies of the instabilities are close to the pump frequency so that we can consider that the dispersion is almost the same for each of them. Therefore, no significant asymmetry can be observed as it has been reported in [18].

To evidence experimentally that our system is convective, we have used a pulsed pump to avoid stimulated Brillouin scattering. The laser emits pulses of 5.5 ps duration with a 20 MHz repetition rate at 1556.1 nm. The fiber ring cavity is composed of 59.5 m of dispersion shifted fiber ($\lambda_0 \simeq 1552$ nm) and 0.5 m of SMF28 ($\lambda_0 \simeq 1300$ nm).

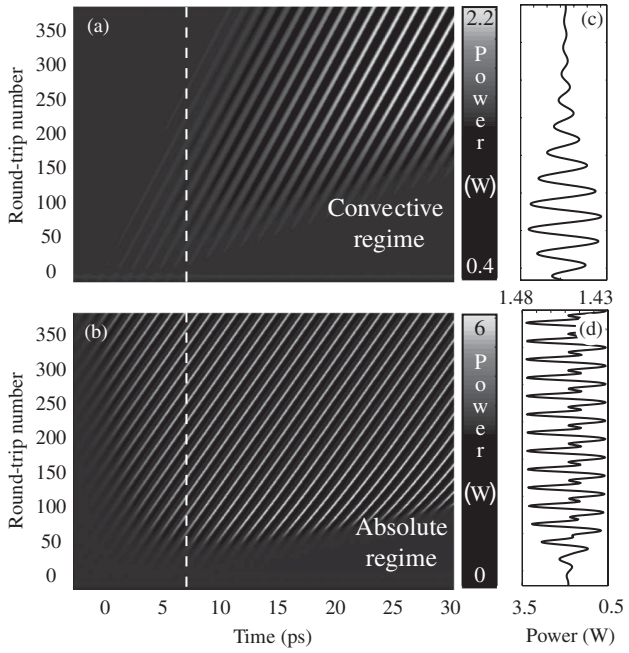

FIG. 3. Evolution of a perturbation initially located at $\tau = 0$ ps and $z = 0$ (round-trip 0) evidencing (a),(c) a convective regime, $P_P = 1.3$ W, and (b),(d) an absolute regime, $P_P = 2$ W. Panels (a) and (b) are the ''pseudospatiotemporal'' slow-fast time evolution maps. Panels (c) and (d) are the slow time evolutions of this perturbation registered at $\tau = 6.5$ ps as indicated by the vertical dashed lines in panels (a) and (b).

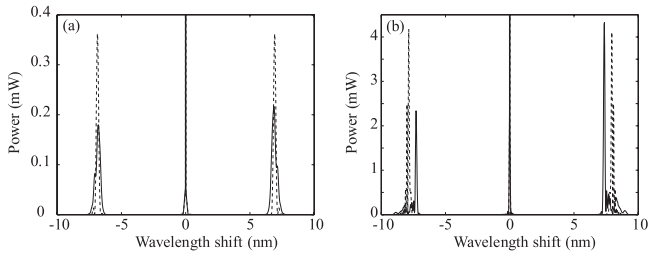

FIG. 4. Numerical solutions of Eqs. (1) and (2) showing the impact of β_3 on the output power spectra after 350 round-trips. Solid (dotted) lines correspond to $\beta_3 = 1.2 \times 10^{-40}$ s^3/m ($\beta_3 = 0$). (a) The convective regime, $P_P = 1.1$ W, and (b) the absolute regime, $P_P = 2$ W. The pump wavelength is located at 1556.1 nm.

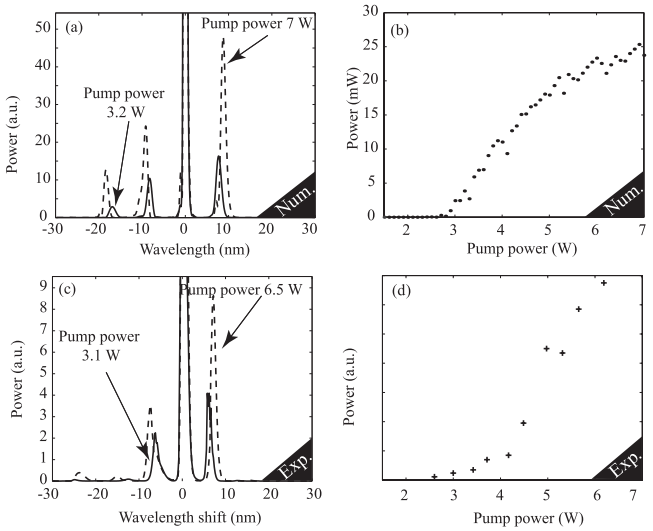

FIG. 5. (a),(c) Numerical and experimental output power spectra for a pulsed pump of 5.5 ps duration. (b),(d) Power difference between the maxima of the two side lobes of modulational instability. (c),(d) Experimental recordings. (a),(b) Numerical simulations taking into account noise. The integrated power spectrum (a) is averaged over the last hundred round-trips to reproduce the experimental averaging coming from the sweep rate time of the optical spectrum analyzer.

At the laser operating wavelength 1556.1 nm, the average second-order dispersion value is approximately $\beta_2 = -5 \times 10^{-28}$ s^2/m and $\beta_3 = 1.2 \times 10^{-40}$ s^3/m. By using a set of an optical delay line and a piezoelectric stretcher (manufactured by LEUKOS), it is possible to control the fiber loop optical path with a submicron accuracy [19]. Care has been given to the synchronization between the pump and the successive pulses having experienced one or more round-trips since synchronization mismatch directly drives the system to be convective [8]. An easy way to achieve it experimentally consists in optimizing the finesse of the cavity by fine-tuning the fiber length. Typical experimental output spectra are displayed in Fig. 5(c) near above the convective threshold (solid line) and well above it (dashed line). They clearly show an asymmetry between the intensities of the two MI side lobes. As predicted numerically for a cw pumping, the MI intensity asymmetry increases with the pump power [Fig. 5(d)]. Numerical simulations carried out for these experimental conditions (pulsed pump plus noise) show a very good qualitative agreement with experiments as can be seen in Figs. 5(a) and 5(b). Thus, the signature found numerically to evidence the convective nature of the system remains valid for pulsed pumps and so forth is relevant. We then conclude that a direct consequence of the symmetry breaking in our fiber system is that it behaves as a convective system, and this is not specific to our system but it is generic to *all fiber systems*.

In summary, we have theoretically and experimentally shown that, in a fiber ring cavity pumped by a pulsed laser, the *third-order dispersion* term breaks the reflection symmetry and leads to the appearance of convective instabilities. More generally, odd-order dispersion terms and the Raman effect in fiber systems correspond to nonlocal terms that make the fiber systems convective. The asymmetry between the two lobes of modulational instability observed in the output power spectrum of fiber systems is a signature of convective instability. A striking feature revealed by our study is that for high enough values of β_3 and pulsed pumping conditions, only noise-sustained modulational instabilities can be observed.

We acknowledge the GDR 3073 PhoNoMi2 and the PAI.

*mussot@phlam.univ-lille1.fr

[1] A. Couairon and J. M. Chomaz, Phys. Rev. Lett. **79**, 2666 (1997); H. R. Brand, D. Deissler, and G. Ahlers, Phys. Rev. A **43**, 4262 (1991); P. Büchel and M. Lucke, Phys. Rev. E **61**, 3793 (2000).
[2] R. J. Briggs, *Electron-Stream Interaction with Plasmas* (MIT Press, Cambridge, MA, 1964).
[3] N. Mitarai and H. Nakanishi, Phys. Rev. Lett. **85**, 1766 (2000).
[4] N. Israeli, D. Kandel, M. F. Schatz, and A. Zangwill, Surf. Sci. **494**, L735 (2001).
[5] O. Nekhamkina and M. Scheintuch, Phys. Rev. E **68**, 036207 (2003).
[6] M. Santagiustina, P. Colet, M. San Miguel, and D. Walgraef, Phys. Rev. Lett. **79**, 3633 (1997); H. Ward, M. Taki, and P. Glorieux, Opt. Lett. **27**, 348 (2002).
[7] E. Louvergneaux, C. Szwaj, G. Agez, P. Glorieux, and M. Taki, Phys. Rev. Lett. **92**, 043901 (2004).
[8] S. Coen, M. Tlidi, Ph. Emplit, and M. Halterman, Phys. Rev. Lett. **83**, 2328 (1999).
[9] G. Agez, P. Glorieux, M. Taki, and E. Louvergneaux, Phys. Rev. A **74**, 043814 (2006).
[10] H. Ward, M. N. Ouarzazi, M. Taki, and P. Glorieux, Phys. Rev. E **63**, 016604 (2000).
[11] R. Zambrini, M. San Miguel, C. Durniak, and M. Taki, Phys. Rev. E **72**, 025603 (2005).
[12] M. Tlidi, A. Mussot, E. Louvergneaux, G. Kozyreff, A. G. Vladimirov, and M. Taki, Opt. Lett. **32**, 662 (2007).
[13] N. Akhmediev, V. I. Korneev, and N. V. Mitskevich, Radiophys. Quantum Electron. **33**, 95 (1990).
[14] Solange B. Cavalcanti, José C. Cressoni, Heber R. da Cruz, and Artur S. Gouveia-Neto, Phys. Rev. A **43**, 6162 (1991).
[15] M. J. Potasek, Opt. Lett. **12**, 921 (1987).
[16] F. Kh. Abdullaev, S. A. Darmanyan, S. Bischoff, P. L. Christiansen, and M. P. Sørensen, Opt. Commun. **108**, 60 (1994).
[17] C. Bender and S. Orszag, *Advanced Mathematical Methods for Scientists and Engineers* (MacGraw-Hill, New York, 1978).
[18] S. Coen and M. Haelterman, Phys. Rev. Lett. **79**, 4139 (1997).
[19] F. Reynaud and E. Delaire, Electron. Lett. **29**, 1718 (1993).